

# From Reaction to Rheology: Linked Molecular Models of Polymerisation Kinetics and Entangled Dynamics Predict Branched Polymer Structure and Flow

Daniel J. Read<sup>2</sup>, Dietmar Auhl<sup>3</sup>, Chinmay Das<sup>3</sup>, Jaap den Doelder<sup>5</sup>, Michael Kapnistos<sup>3</sup>, Iakovos Vittorias<sup>4</sup>, Tom C. B. McLeish<sup>1</sup>

<sup>1</sup>*Departments of Physics and Chemistry, Durham University, Durham, DH1 3LE, UK*

<sup>2</sup>*Department of Applied Mathematics, University of Leeds, Leeds, LS2 9JT, UK*

<sup>3</sup>*Department of Physics and Astronomy, University of Leeds, Leeds, LS2 9JT, UK*

<sup>4</sup>*Basell Polyolefine GmbH, R&D Polymer Physics and Characterization, Frankfurt, Germany*

<sup>5</sup>*Dow Benelux B.V., Polyethylene Product Research, P.O. Box 48, 4530 AA, Terneuzen, The Netherlands*

**We present a predictive scheme connecting the topological structure of highly branched entangled polymers, with industrial-level complexity, to the emergent viscoelasticity of the polymer melt. The scheme is able to calculate the linear and non-linear viscoelasticity of a stochastically branched “high-pressure free radical” polymer melt as a function of the chemical kinetics of its formation. The method combines numerical simulation of polymerisation with the tube/entanglement physics of polymer dynamics extended to fully non-linear response. We compare calculations for a series of low-density polyethylenes (LDPE), with experiments on structural, and viscoelastic properties. The method provides a window onto the molecular processes responsible for the optimized rheology of these melts, connecting fundamental science to process in complex flow, and opens up the *in silico* design of new materials.**

One of the long-standing fundamental challenges to soft matter science is the quantitative connection between molecular topology and dynamics of branched entangled polymers. The motivation arises from both the universality of the physics (1) and the experimental and engineering properties of highly branched polymers (2). Very slow dynamical processes, on timescales of many seconds, emerge even when the entangled macromolecules are of simple linear topology. The additional complication of branching extends the range of relaxation times exponentially, and generates additional elasticity in the response to strong extensional flow (3). A quantitative account of these phenomena has emerged for very simple polymer structures, but has remained elusive in highly complex blends arising from statistical polymerisation processes arising in industry (4).

The most successful theoretical approach to entangled polymer dynamics is the “tube model” of Doi, Edwards and de Gennes (5,6). The model supposes that the topological constraints on any given chain from its neighbors are equivalent to those of a tube around the chain contour. So polymer chains are free to move tangentially their local contours, but, beyond a characteristic “tube diameter”, not perpendicular to them. New configurations are always generated by chain ends, as these may explore the surrounding field of chains without constraint. Adding thermal motion to this simple picture immediately predicts qualitatively different dynamics for linear and branched chains. Linear chains diffuse simple curvilinear diffusion (“reptation”) along the tube contour. The orientational configuration of a chosen chain is essentially re-equilibrated by reptation out of its original tube into a new one, a process dominated by a single “reptation time”. On the other hand, in branched polymers, reptation is highly suppressed and new configurations of the chains can only be achieved by an exponentially-slower “arm retraction” mode (7). In this case the chain reconfiguration occurs hierarchically, beginning rapidly at the extremities of entangled arms, and ending at segments adjacent to the branch points. These are visited by retracting chain ends only exponentially rarely, so giving rise to a wide range of experimental relaxation times along the whole entangled arm. Experiments on well-characterised star-polymer melts confirmed such extreme slowing down in both diffusion (8,9) and rheology (the stress/strain-rate relations that control fluid flow) (10). The universal topological nature of the tube theory allows quantitative mapping of its predictions to any particular polymer chemistry and temperature *via* just two parameters: (i) the “plateau modulus”  $G_0$ , which controls the level of elastic stress supported by the melt and which depends on the tube diameter: (ii) the entanglement time  $\tau_e$ , which sets the timescale of the fastest entangled viscoelastic mode.

Theory and experiment have since been extended to more complex single-molecule topologies: H-shapes (11), combs (12), and multi-arm polymers (13,14), confirming the predictions of universality over chemistry, and the central role of molecular topology. The hierarchical relaxation of entangled star polymers generalises to more complex architectures: once free ends retract back to the outermost layer of branch-points, these become mobile, activating deeper retractions towards the second layer, and so on (15). The relaxation time of a given tube segment in an ensemble of branched polymers depends on the curvilinear distance to the free end that eventually retracts and disentangles it, and on the dangling trees attached to this path that slow down the retraction process (see Figure 1). The prediction of the linear stress-relaxation response of a complex melt therefore reduces to the calculation of the relaxation times by arm retraction of all the segments within it, a programme that has been carried through in the case of the simplest cases of polydisperse branched polymers generated by “metallocene” catalysts (16).

The tube theory also makes predictions for strongly non-linear response. In strong flows, the “buried” segments of a highly branched polymer can stretch just as they would in an elastic network. The distinction of the fluid melt is that this stretch must be bounded. This non-linear bound on segment stretch is controlled, not by the relaxation time statistic, but by the number of free-ends connected to it. Termed the “priority”, it increases rapidly with depth into a highly branched polymer (15,17). Figure 1 indicates by example the segment depth and priority values of segments within a typical complex molecule.

In spite of this progress, a predictive scheme for even the most common industrial polymers, that connects the molecular structure developed in a reactor to the full linear and non-linear rheology of the emergent melt, has remained out of reach. We now have all the ingredients to bridge this gap. We connect the output of a model for industrial LDPE polymerization (4) to a numerical algorithm (17) that captures all the relevant entangled polymer dynamics, enhanced with a non-linear calculation of priority as well as relaxation time statistics, making predictions for a range of intensively characterized industrial materials.

We model the LDPE polymerisation process by adapting the original algorithm of Tobita (3) to produce by Monte Carlo simulation a data structure that can be read by a tube-model calculation. The algorithm is based upon a set of processes occurring in a batch reactor during free-radical polymerisation: initiation of free radicals (rate  $R_i$  per unit volume); propagation or polymerisation (rate  $R_p$ ); termination by disproportionation (rate  $R_{td}$ ) and combination (rate  $R_{tc}$ ); chain transfer by long-chain branching (rate  $R_b$ ), to small molecules (rate  $R_f$ ) and by scission (rate  $R_s$ ). Under steady-state conditions there emerge five independent parameters that determine the resulting polymer architecture for any set of reaction conditions. These are: the total conversion  $x_f$  of monomer to polymer and the dimensionless rates of termination ( $\tau$ ), combination ( $\beta$ ), branching ( $C_b$ ) and scission ( $C_s$ ) made dimensionless by the propagation rate:

$$\begin{aligned}\tau &= (R_{td} + R_f) / R_p \\ \beta &= R_{tc} / R_p \\ C_b &= k_b / k_p \\ C_s &= k_s / k_p\end{aligned}\tag{1}$$

These five parameters set the topological admixture and overall molecular weights of the melt resulting from a single batch process. Increasing  $\tau$  or  $C_s$  results in shorter chain strands and smaller overall molecular weight. Increasing  $\beta$  increases molecular weight and polydispersity, but without greatly affecting branch density or typical strand length between branchpoints. Increasing  $C_b$  increases branching, molecular weight and polydispersity, but reduces the strand

length. The natural distribution in reactor residence times  $x_f$  is modelled by a weighted sum over simulations of two or three values of  $x_f$  to match the molecular weight distribution of a single tubular-reactor LDPE resin.

A second algorithm then applies the two fundamental processes of reptation and arm retraction to the numerical polymer ensemble (17). It recognises that, at longer timescales, the relatively rapidly-relaxing outer parts of the molecules are no longer effective at entangling the deeper strands, so that the effective tube constraints widen for deeper segments, and the topologies of the molecules simplify (see Figure 1).

To predict the full non-linear response we map the priority and relaxation time distributions onto “pom-pom” modes, a model derived from the tube physics for an entangled strand trapped between two branch points (18,19). Each strand mode  $i$  is accorded a (slow) orientation time,  $\tau_{io}$ , a (faster) strand stretch time  $\tau_{is}$ , and a strand “priority”  $q_i$  which sets the maximum extent of its possible stretch in a fast flow.

The physics of hierarchical relaxation generates, beginning at each free chain end, a relaxation coordinate  $z(t)$  moving inwards towards the deeper segments of the molecule. The orientational relaxation time  $\tau_{io}$  of a segment is just that at which the relaxation front reaches it. In a similar way the faster segmental stretch times  $\tau_{is}$  are set by a second inward-travelling front  $\tilde{Z}(t)$  (17). To assign the segment priorities,  $q_i$ , we recognise that the values generated by the simple end-counting procedure described above, and in Figure 1, are valid only when all segments are maximally stretched (at very high flow rates). At lower flow rates, the effective priority of a strand is calculated by propagating the steady-state values of segmental tension for that rate onto the segment from its connected free ends, noting that a segment can only stretch if the flow rate exceeds the inverse of its stretch relaxation time. This is essential physics to capture, as we know from experiments on controlled-architecture melts (11).

For consistency with the linear rheology predictions we actually need two sets of pom-pom modes associated with each strand. They correspond to stress relaxation *via* entanglement escape of strands; the second set corresponds to the consequent stress relaxation in neighbouring strands of longer relaxation time (17).

We have obtained, from the two different companies in our collaboration, commercial LDPE materials generated in tubular reactors which were analysed with GPC-MALLS (Gel-Permeation-Chromatography coupled with Multi-Angle-Laser-Light-Scattering) and subsequently measured the linear and non-linear rheology (material data are given in SOM). These techniques give two measures of the molecular weight distribution (MWD). Firstly the weight of material in each

fraction gives the (MWD) itself. Secondly, light-scattering on each fraction gives the mean solution radius of gyration of its molecules. This is usually expressed as a fraction of the radius of gyration of a linear polymer of the same molecular weight in the same solution. Termed the “g-factor”, it is a measure of the degree of branching: the more branch-points within the molecule, the more compact its size in solution. Both MWD and  $g(M)$  can also be calculated from our numerical ensemble. This allowed us to iterate the parameters of the polymerisation model for each material until we found a theoretical LDPE ensemble consistent with both functions (parameters in SOM). In Figure 2(a) we give a typical example (for LDPE2). The MWDs are captured very well by the fits. We set  $C_s = 0$  throughout, since its value appeared to be consistently small when left as a free parameter. The termination-rate parameter  $\tau$  controls the low weight tail of the MWD, while its breadth could be increased by increasing either  $\beta$  or  $C_b$ . Increasing the ratio  $\beta/C_b$  tended to result in more sparsely branched molecules (thus increasing  $g(M)$ ). Increasing the conversion  $x_s$  amplified the effects of both  $\beta$  and  $C_b$ . A reasonable fit could be obtained by combining a high-conversion fraction (which provides the high molecular weight tail) with one or two lower conversion fractions (filling out the MWD at lower molecular weight). We found the expected underdetermination of the complex set of structure parameters from static structure parameters alone. This is one of the motivations of a quantitative molecular calculation of the more sensitive rheological response.

Fixing the two relevant tube model parameters of  $G_o$  and  $\tau_e$  (rheological material parameters and methods are given in SOM), and taking numerical blends consistent only with MWD and  $g(M)$  allowed initial prediction of their linear rheology curves within roughly half a decade. As expected from the greater sensitivity of the rheology to branched structure, small adjustments to the reaction parameters (resulting in almost indistinguishable results for MWD and  $g(M)$ ) could then be made so as to fit the linear rheology: these are the results in Figure 2 (lower panel). This is a remarkable indication of the success of our methodology: because of the exponential dependence of rheological relaxation times on branch length, predictions of this type can easily be orders of magnitude from data. The results also confirm that even the dense branching of LDPE permits a theoretical treatment using tube-theory; even subtle features such as the cross-over frequencies of in-phase and out-of-phase responses are accurate. Only a very small weight of very slow modes appears in the model but not in the data.

With no further adjustment of the reaction scheme or rheological parameters at all, we calculated the non-linear transient response in strong shear and extension of the test materials. Theoretical predictions and experimental data are given over a wide range of deformation rates in Figure 3 for the first three samples. Using the new algorithm for assigning effective segment priorities, for all three melts the technologically essential extensional response is predicted with

remarkable accuracy. The onset, slope and maximum of the extensional hardening are consistent with the data in each case (note that for the higher molecular weight (LDPE 2 and 3) materials, the extensional sample always breaks before the maximum stress is reached). Crucially we also capture in the case of LDPE1 the rate at which hardening sets in (as well as its much reduced scale). In shear the model predicts the existence and position of a transient stress maximum in each case, and the qualitatively different “thinning” behaviour in contrast to the “hardening” in extension.

The successful non-linear predictions are surprising: the phenomenon is highly-sensitive to details of the long chain branching still underdetermined by the solution measurements and linear rheology. Might the non-linear predictions be fortuitous, and other numerical ensembles equally consistent with the linear measurements give radically different non-linear predictions? We tested this by constructing examples of these alternative distributions. The dashed curves in Figure 3 for LDPE 2 show the extensional and shear predictions for an ensemble constructed from a blend of two, rather than three degrees of conversion (parameter values in SOM). MWD,  $g(M)$  and linear rheology are essentially identical, but the reaction parameters in the two fractions differ markedly from any of the three in the first model. Yet we see that the non-linear predictions are robust. But the reason for this commercially vital feature is subtle: it is sensitive to the branched structure only through the relaxation time/priority distribution. Providing this is correct, variations in structure within that ensemble will not result in variation of rheological response. The additional constraints from the polymerisation scheme are sufficient to ensure that the ensemble belongs to the correct region of relaxation time/priority space. Figure SOM1 in the shows an example of a time-dependent correlation map of relaxation time and priority (for LDPE1). It also indicates the two extreme structures of perfect combs and perfect Cayley trees which constitute bounds for such maps. At the earliest time the outer structures and lowest molecular weights resemble comb-like topologies, but at longer times the larger structures acquire a more ramified topology of branching, although an important finding is that the ensemble is always very far from being accurately represented by Cayley trees (20).

We are now in a position to start exploring hypothetical variations in reaction conditions with a view towards molecular design of new melts. We chose to tackle the important question of independent tuning of the linear and non-linear rheology, and created different single-batch ensembles (see Table 1) with near-identical linear rheology.

Resin	$T$	$\beta$	$C_b$	$C_s$	$x_{sI}$	$w_I$
BATCH1	$1 \times 10^{-3}$	$8 \times 10^{-5}$	$2 \times 10^{-2}$	0	0.15	1
BATCH2	$8.5 \times 10^{-4}$	$8 \times 10^{-5}$	$5 \times 10^{-3}$	0	0.15	1

Table 1: The reaction model parameters of the hypothetical materials

The predicted MWD, branching structure and linear rheology spectrum for the two melts are shown in Figure 4. Also shown is the predicted transient response in strong extension of two resins. The first is predicted to show much stronger extension hardening (similar in magnitude to LDPE2 and 3) than the second (similar to LDPE1). This is a result of its higher degree of branching (larger  $C_b$ ), compensated in the second by a smaller strand molecular weight (the parameter  $\tau$  is also larger for melt 1). This example serves to illustrate that, by separately controlling the degree of branching and strand molecular weight, independent control can in principle be exercised over the linear rheology and extension hardening of LDPE resins: this is a vital principle for design of custom materials.

## References

1. P.-G. De Gennes, *Scaling Concepts in Polymer Physics*, Cornell (1980).
2. P.A. Small, Long chain branching in polymers. *Adv. Polym. Sci.* **18**, 1 (1975).
3. J.M. Dealy and R.G. Larson, *Structure and Rheology of Molten Polymers*, Hanser (2006).
4. H. Tobita, Simultaneous long-chain branching and random scission: I Monte Carlo simulation. *Journal of Polymer Science Part B*, **39**, 391-403 (2001).
5. M. Doi and S. F. Edwards, *The Theory of Polymer Dynamics*, Oxford (1986)
6. P.-G. De Gennes, Reptation of a polymer chain in presence of fixed obstacles. *J. Chem. Phys* **55**, 572-579 (1971).
7. P.-G. De Gennes, Reptation of stars. *J. Phys. (Paris)* **36**, 1199-1203 (1975).
8. J. Klein *et al.*, Diffusional behaviour of entangled star polymers. *Nature*, **304**, 526-527. (1983).
9. K.R. Shull, *et al.* Effect of number of arms on diffusion of star polymers. *Nature*, **345**, 790-791. (1990).
10. D.S. Pearson and E. Helfand, Viscoelastic properties of star-shaped polymers. *Macromolecules*, **19**, 888-895 (1984).
11. T.C.B. McLeish *et al*, Dynamics of Entangled H-Polymers: Theory, Rheology and Neutron-Scattering. *Macromolecules*, **32**, 6734-6758 (1999).
12. N.J. Inkson, R.S. Graham, T.C.B. McLeish, D.J. Groves, C.M. Fernyhough, Viscoelasticity of monodisperse comb polymer melts. *Macromolecules* **39**, 4217-4227 (2006).

13. Juliani and L.A. Archer, Relaxation Dynamics of Entangled and Unentangled Multiarm Polymer Solutions: Comparisons with Theory. *Macromolecules* **35**, 10048–10053 (2002).
14. E. van Ruymbeke, *et al.* Entangled dendritic polymers and beyond: rheology of symmetric Cayley-tree polymers and macromolecular self-assemblies. *Macromolecules* **40**, 5941–5952 (2007).
15. T.C.B. McLeish, Tube theory of entangled polymer dynamics. *Adv. Phys.*, **51** 1379-1527 (2002).
16. C., Das *et al.*, Computational linear rheology of general branch-on-branch polymers, *J. Rheol.* **50**, 207-234 (2006).
17. T. C. B. McLeish and D. K. Bick, Topological Contributions to Non-linear Elasticity in Branched Polymers. *Phys. Rev. Letts*, **76**(14), 2587-2590, (1996)
18. T. C. B. McLeish and R. G. Larson, Molecular Constitutive Equations for a Class of Branched Polymers: The Pom-Pom Polymer. *Journal of Rheology*, **42**, 1, 81-110, (1998).
19. R.J. Blackwell *et al.*, Molecular Drag-Strain Coupling in Branched Polymer Melts. *J. Rheol.*, **44**, 121-136 (2000).
20. P., Stanescu *et al.*, Modeling of the linear viscoelastic behavior of low-density polyethylene. *J. Polym. Sci. B*, **43**, 1973-1985 (2005).

## Acknowledgments

We thank EPSRC (UK) for funding under the “Microscale Polymer Processing” (MuPP) consortium and the EU FPVII People Programme for funding under the Marie Curie Initial Training Network DYNACOP. The data described in this work are archived on the MuPP project online materials database at <http://www.irc.leeds.ac.uk/mupp2/>

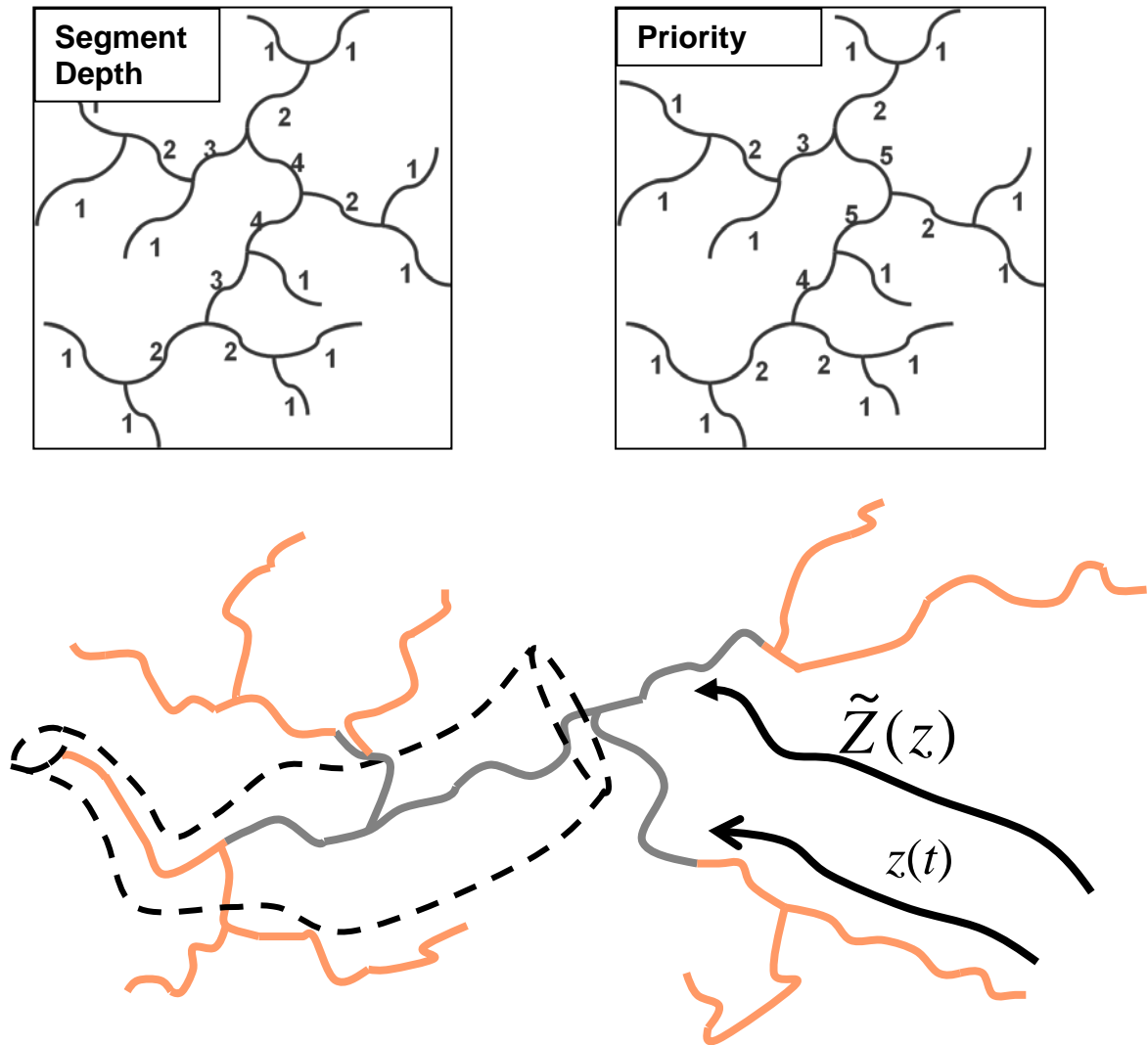


Figure 1

Upper panel: discrete values of the segment depth (controlling relaxation time) (left) and priority (right) values for segments in an arbitrarily chosen branched polymer.

Lower panel: A typical branched molecule within a branched ensemble undergoing configurational relaxation after a step strain at time  $t$ . The co-ordinate  $z(t)$  divides a branch into relaxed ( $z < z(t)$ ) and unrelaxed ( $z > z(t)$ ) portions. The co-ordinate  $\tilde{Z}(z)$ , also increasing with  $t$ , indicates the effective root at time  $t$  of the branch relaxing the front at  $z(t)$ . On the branch at the left is indicated the increasing effective tube diameter for deeper segments as the entanglement network dilutes.

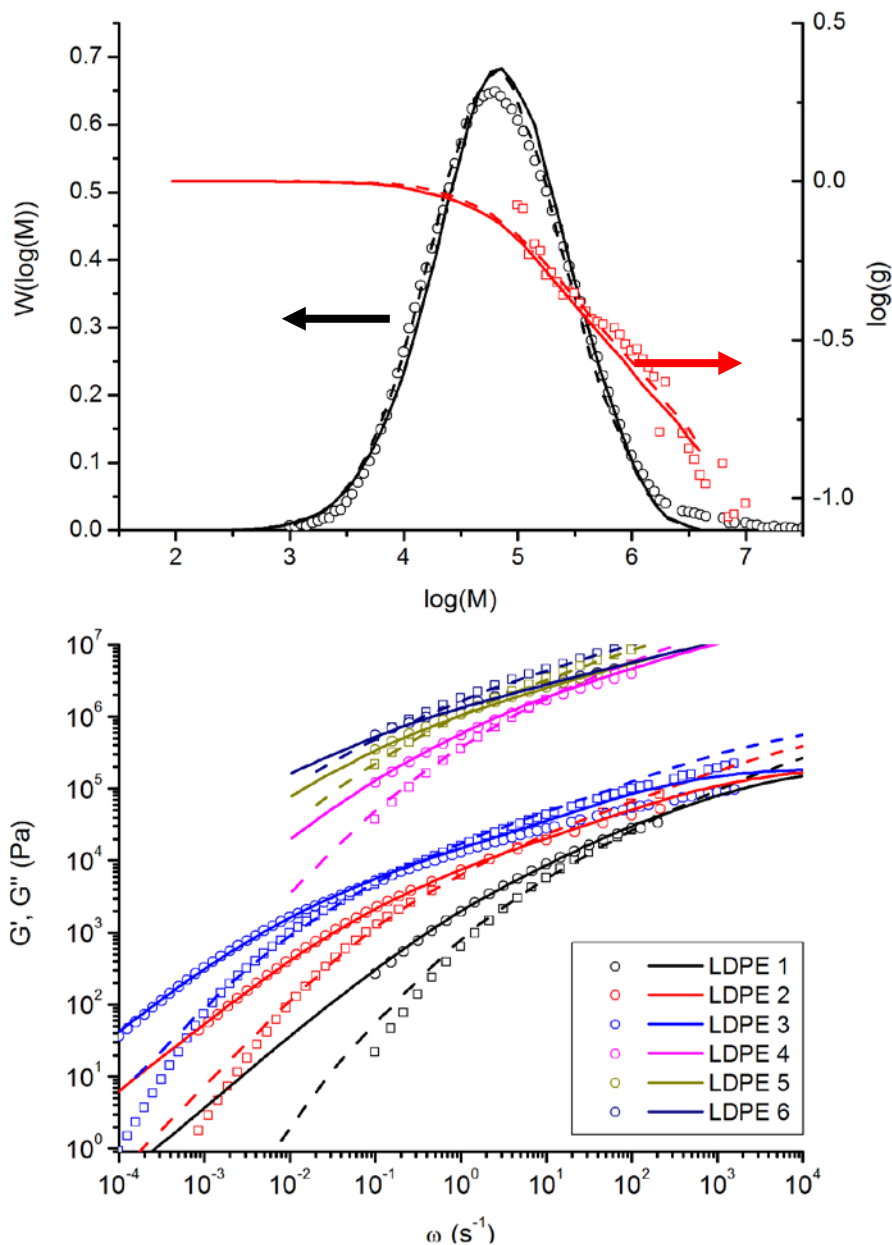


Figure 2

(Upper) Example of simultaneous fit of the reaction scheme to the molecular weight distribution (black) and branching factor  $g'(M)$  (red) for the sample LDPE2.

(Lower) Linear rheological response of the LDPE materials in the frequency domain showing in phase ( $G'(\omega)$  : dashed lines / squares) and out of phase ( $G''(\omega)$  : solid lines / circles) components of stress. In each case data are points and the model results smooth curves. Samples 4, 5 and 6 are shifted upwards by 2 decades for clarity.

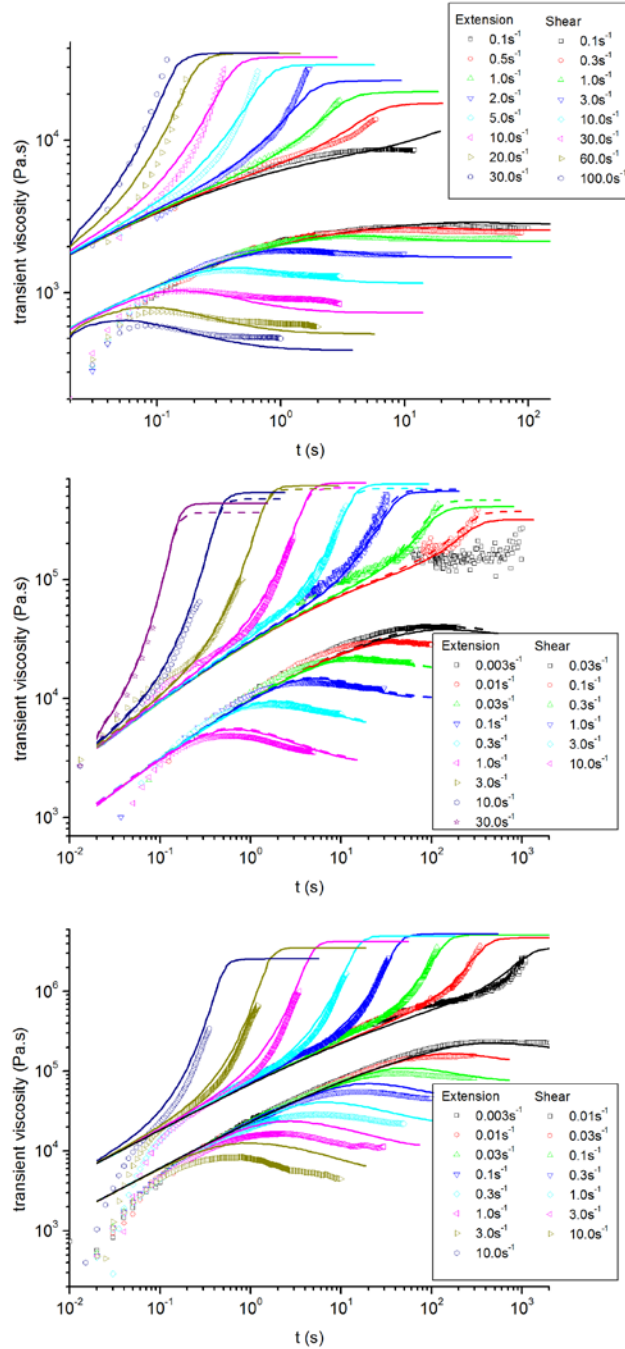


Figure 3

Non-linear transient viscosity growth curves in uniaxial extension (upper curves) and shear (lower curves) for (top) LDPE1, (middle) LDPE2, (bottom) LDPE3. The temperature is 150°C. Rates range from  $0.003\text{s}^{-1}$  to  $100\text{s}^{-1}$  and as shown on the plots. Data are symbols; the parameter-free model predictions are solid curves. The dashed curves for LDPE2 show the predictions of an alternative bimodal (rather than trimodal) numerical polymerisation ensemble, equally consistent with solution measurements and linear rheology, and indicative of the robustness of the scheme to fine details of molecular ensemble once relaxation time and priority structures are correct.

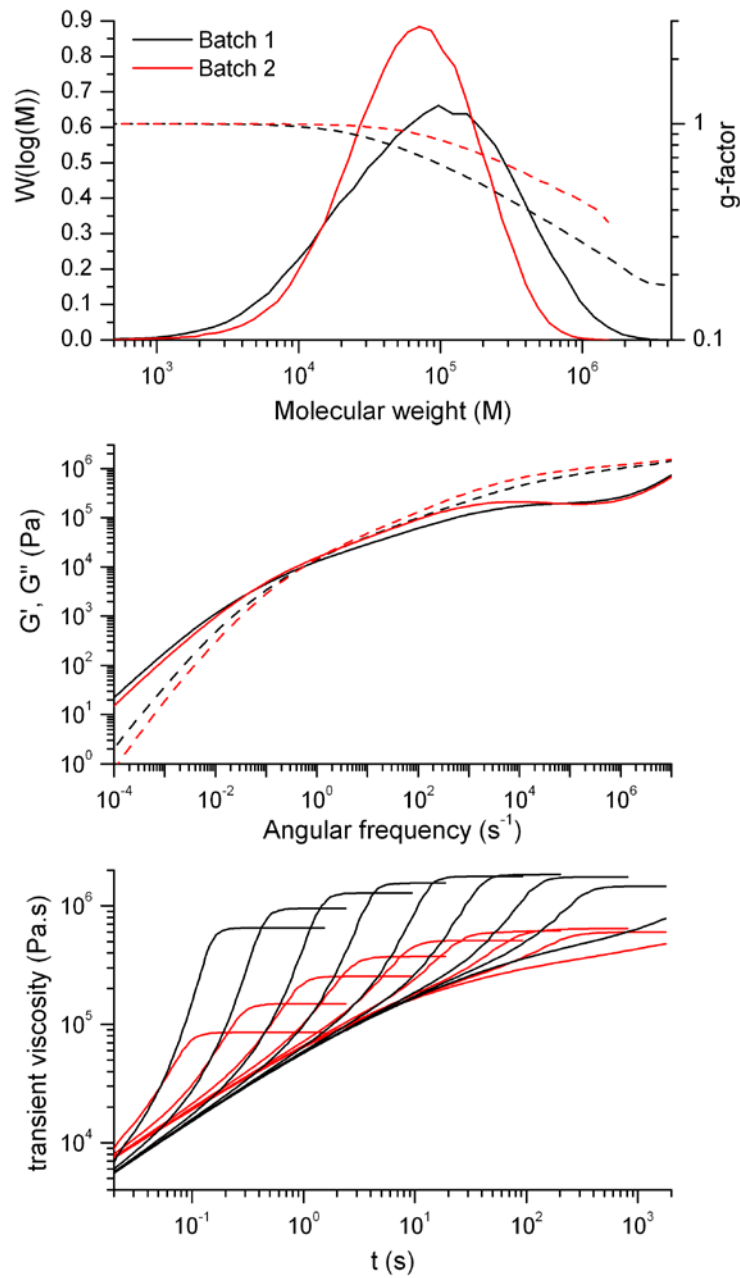


Figure 4

Two reaction models (Batch 1, Batch 2) with the parameters as in Table 1 were used to calculate Upper: molecular weight (and branching;  $g$ ) distributions; Middle: linear rheology (solid curves are  $G''$ , dashed curves  $G'$ ) and Lower: extensional rheology at a range of rates (black curves are Batch 1, red curves are Batch 2). All rheology calculations use the parameters from Table 2. Although they have very similar linear rheology, this has been achieved through different combinations of branching and molecular weight distributions. As a result, the degree of extension hardening for the two hypothetical resins is quite different.